Effect of partial crystallization on the structural and Er3+ luminescence properties of phosphate-based glasses

C. Gestraud, Benoit Glorieux, Jonathan Massera, Laëtitia Petit, Alexandre Fargues, Marc Dussauze, Thierry Cardinal, Leena Hupa

Effect of partial crystallization on the structural and Er^{3+} luminescence properties of phosphate-based glasses

C. Gestraud[1,2], B. Glorieux[2], J. Massera[1, 3], L. Petit[1,4*], A. Fargues[2], M. Dussauze [5], T. Cardinal[2], L. Hupa[1]

[1] *Johan Gadolin Process Chemistry Centre, Åbo Akademi University, Biskopsgatan 8, FI-20500, Turku, Finland*

[2]*CNRS, Université de Bordeaux, ICMCB, 87 Avenue du Dr Schweitzer, F-33608 Pessac, France*

[3]*Tampere University of Technology, Department of Electronics and Communications Engineering, Korkeakoulunkatu 3, FI-33720 Tampere, Finland.*

[4]*Optoelectronics Research Centre, Tampere University of Technology FI-33101 Tampere, Finland*

[5]*Institut des Sciences Moléculaires, CNRS UMR 5255, Université de Bordeaux, 33405 Talence, France*

** Corresponding author:laeticia.petit@tut.fi*

Abstract

In this paper, the impact of B_2O_3, ZnO and TiO_2 addition on the structure, Er^{3+} luminescence and crystallization of glasses in the Er_2O_3-P_2O_5-CaO-SrO-Na_2O glass system is reported. The thermal properties of the as-prepared glasses were recorded using a DTA and the structure of the glasses prior to and after heat treatment was analyzed using Raman and IR spectroscopies. Crystallization of the glass after heat treatments was confirmed by the presence of sharp peaks in the XRD patterns. Based on the XRD pattern, two different crystalline phases are suspected to precipitate, the composition of which depends on the glass composition. From the spectroscopic properties of the glasses, the Er^{3+} ions are not suspected to be incorporated in the crystals.

Key words: Er doped glasses, heat treatment, nucleation and growth, micro-Raman & Infrared spectroscopies, Er luminescence properties

1. Introduction

Glasses and glass-ceramics doped with rare-earth (RE) ions have been intensively studied for their use in telecommunications systems, such as up-converter, fibers, optical amplifiers, solid state lasers and 3D displays [1]. Among the RE ions, Er^{3+} doped materials have attracted great interest because of their potential applications as optical fiber amplifiers due to their ability to increase the signal at the wavelength of 1530nm, which corresponds to the intra-4f transition of Er^{3+} from $^4I_{13/2}$ to $^4I_{15/2}$ [2]. Oxide glasses have been found to be stable hosts for obtaining efficient luminescence from RE ions [3].

In the development of optical devices containing rare-earth (RE) ions, the optical properties are mainly determined by the local environment around the RE [4]. Locally ordered nuclei of $ErPO_4$ were found to form in germano-silicate glasses and exhibit luminescence properties typical of RE-doped crystals [5]. Those nanometer-sized particles in glass are of great interest as they offer promising perspectives in terms of resolution and luminescence efficiency [6]. Additionally, the photoluminescence intensity of phase separated Er^{3+} doped sodium borosilicate glass was found to be higher than that for the as-prepared glasses [7]. In this glass system, the phase separation led to a borate phase and a silicate phase, the Er^{3+} ions being segregated into the borate-rich phase. The work on the processing of glass-ceramics with nanoparticles small enough to avoid strong light scattering and with rare-earth ions incorporated into a crystalline phase, has recently opened a new route to increase the efficiency of glass as active hosts [8]. Those new glass-ceramic materials combine some features of glasses (easier and cheaper processing than for single crystals) and some advantages of rare-earth doped single crystals (higher absorption/emission cross-section and longer lifetime of luminescent levels) [9].

The crystallization behavior of phosphate-based glasses with composition $50P_2O_5$-(40-x)CaO-xSrO-$10Na_2O$ with x=0, 20 and 40 (in mol%) was reported recently [10]. Two phases crystallized in the glasses: $Ca(PO_3)_2$ and $NaCa(PO_3)_3$ in the glass with x=0, $Sr(PO_3)_2$ and $NaSr(PO_3)_3$ in the glass with x=40 and a solid solution of $(Ca,Sr)(PO_3)_2$ and $Na(Ca,Sr)(PO_3)_3$ in the glass with x=20. All crystals were found to preferentially nucleate and grow from the surface. In order to increase the tendency of the glass to crystallize, nucleation agent can be added in the glass network. Previous studies have revealed that B_2O_3, TiO_2 or ZnO can act as good nucleation agent in many glasses [11-12]. The role of those elements as nucleation agent in phosphate glasses has not been fully studied. Additionally, to the best of our knowledge, there is only little

information on understanding the impact of the nucleation and growth of phosphate glasses on Er^{3+} spectroscopic properties.

Therefore, in this study, we focused on the understanding the influence of these elements introduced in low concentration (<5mol%) on the structure and crystallization behavior of the glasses. We also checked the impact of the glass crystallization on the luminescence properties of erbium. Our main goal of this study will be to process a phosphate glass which upon heat treatment exhibits a volume crystallization associated with the precipitation of evenly distributed Er^{3+} doped nanocrystals. In this paper, different Er^{3+} doped phosphate glasses within similar glass system (P_2O_5-CaO-SrO-Na_2O) were heat treated at different temperatures in order to study the spectroscopic properties of the (partially to fully) crystallized glasses. The changes of the structure and luminescence properties were investigated.

2. Experimental

2.1 Glass preparation

Glasses with the composition 100-x(0.5P_2O_5-0.2SrO-0.2CaO-0.1Na_2O)-0.0025Er_2O_3-xB_2O_3/TiO_2/ZnO (x=0, 2.5 or 5) (mol %) were studied. B_2O_3 and ZnO were added within 2.5 mol% (the glasses were labeled B-Er and Zn-Er glasses) while 2.5 and 5mol% of TiO_2 were used (the glasses were labeled Ti2.5-Er and Ti5-Er glasses). The glass with x=0 is labeled as Reference-Er glass. The glasses were prepared using $NaPO_3$ (Alfa Aesar, ACS Reagent), $SrCO_3$ (Sigma-Aldrich, ≥99.9%), $CaCO_3$ (Sigma-Aldrich, ≥99.0%), Er_2O_3 (MV LABORATORIES,INC., 99.999%), H_3BO_3 (Sigma-Aldrich, ≥99.5%) or TiO_2 (Sigma-Aldrich,99-100.5%) or ZnO (Sigma-Aldrich,≥99.0%) and using standard melting method in silica crucible. First, $Ca(PO_3)_2$ and $Sr(PO_3)_2$ were elaborated by mixing $CaCO_3$ or $SrCO_3$ with $(NH_4)_2HPO_4$ (Merck, ACS Reagent). These precursors were then used in combination with $NaPO_3$, Er_2O_3 and H_3BO_3 or TiO_2 or ZnO to prepare the final glass. The raw materials were ground and mixed to prepare a 25g batch, then placed in a silica crucible and melted at 1100°C for 45min. After quenching, the glasses were annealed for 4h at 40^{o}C below their respective T_g to remove the internal stress induced by the quenching. Finally, the glasses were cut and polished, or ground depending on the experimental characterization targeted. All the glasses have a slight pink coloration except the Ti-containing glasses which have a dark pink coloration. X-ray

measurements performed on all as-prepared glasses did not show diffraction peaks, characteristic of the amorphous state of the as-prepared glasses.

The glass compositions were checked by using a Scanning Electron Microscope (Leo 1530 Gemini, Zeiss) coupled with an Energy Dispersive X-Ray Analyser (SEM/EDXA) (Vantage by Thermo Electron Corporation).

The investigated glasses were polished and then heat treated first at T_g+20°C for 6 and 17 h to form nuclei and then at T_p-40°C for 10 to 60 min to grow the nuclei into crystals. The duration of the heat treatments was chosen based on the study of the crystallization mechanism of the glasses with the composition $50P_2O_5$-(40-x)CaO-xSrO-$10Na_2O$ (in mol%) with x=0, 20 and 40 [10]. The polished glass pieces were placed on a platinum foil to prevent contamination from the sample holder. The heat treatments were performed in air.

2.2 Thermal and physical properties

The glass transition temperature (T_g) and crystallization temperature (T_p) were measured by differential thermal analysis (STA449 F1 JUPITER from Netzsch) at the heating rate of 10 ^oC/min. The T_g was taken at the inflection point of the endotherm, as obtained by taking the first derivative of the DSC curve. T_p was defined as the maximum of the exothermic peak. The temperatures were determined with an accuracy of ±3 ^oC.

The density of the bulk glass materials was measured after Archimedes' method in water. The accuracy was better than ±0.02g/cm^3.

2.3 Optical properties

The UV-visible-IR absorption spectra of the glass samples were recorded using a Perkin Elmer Lambda 900 UV-vis-NIR spectrometer with an integrating sphere setup over the 250-2500 nm spectral region. The measurements were performed at room temperature and were corrected for the Fresnel losses and the glass thickness. The absorption cross-sections (σ_{abs}) were calculated from the experimentally measured absorption coefficients and from Er^{3+} ions concentration in the glass, using Equation (1).

$$\sigma_{abs}(\lambda) = \frac{\ln 10}{NL} \log\left(\frac{I_0}{I}\right) \quad (1)$$

where $\log(I_0/I)$ is the absorbance, N the rare-earth ion concentration (ions.cm^{-3}) calculated from the batch composition and the glass density and L the thickness of the sample (cm).
The absorption spectra over the 2500-4000 cm^{-1} range were performed on a FTIR Bruker Alpha-T spectrometer with a spectral resolution of 2 cm^{-1}. The measurements were performed at room temperature and were corrected for the Fresnel losses.

The emission spectra in the 1400-1700 nm range were measured with an Edinburgh Instruments monochromator (M300) and a liquid nitrogen cooled germanium detector (ADC 403L) at room temperature using an excitation source emitting at 980 nm.

2.4 Structural properties

The crystalline phases were identified using an X-ray diffraction analyzer (Philips X'pert) with Cu Kα radiation (λ= 1.5418 Å). The scans were performed from 2θ = 0 to 60° with a step size of 0.02°.

Raman spectra were recorded with a Xplora Horiba micro-Raman spectrometer using a 785 nm excitation line with 10 mW of incident power. Raman spectra in the range of 200–2000 cm−1 were recorded with a resolution of 2.5 cm−1.

The Attenuated Total Reflectance Infrared spectra were recorded on a Thermo Scientific Nicolet iS50 FT-IR spectrometer equipped with a DLaTGS detector (KBr window) using the diamond iS50 ATR accessory. Each spectrum was obtained in the 4000−400 cm−1spectral range, at a resolution of 4 cm−1, by co-adding 200 scans.

3. Results and discussion

The goal of this work is to investigate the effect of nucleation and growth on the structural and Er^{3+} luminescence properties of phosphate-based glasses prepared with different dopants: 2.5 mol% of B_2O_3 and ZnO were added in glasses (the glasses were respectively labeled B-Er and Zn-Er glasses) while 2.5 and 5mol% of TiO_2 were used (the glasses were labeled Ti2.5-Er and Ti5-Er glasses).

3.1 Effect of the glass composition on the thermal, structural and luminescence properties

The density of the glasses and some of their thermal and optical properties are listed in Table 1. The addition of B_2O_3, TiO_2, and ZnO leads to a slight increase in the glass density. This could be attributed to the smaller ionic radius of B, Ti and Zn as compared to the ionic radius of the other elements in the glasses, which has an influence on the compaction of the network. The addition of ZnO reduces T_g and T_p whereas the addition of B_2O_3 and TiO_2 increases T_g and T_p. The increase in T_g could indicate that the addition of B_2O_3 and TiO_2 improves the strength of the network whereas the reduction in T_g for the glass containing ZnO indicates that ZnO acts as a network modifier, in agreement with [13]. Table 1 shows also ΔT, the temperature difference between T_g and T_p. Typically, a large ΔT value is an indication of a small probability for overlapping between the nucleation and growth curves. While the addition of ZnO increases ΔT, the addition of B_2O_3 does not have any significant impact on ΔT. However, the addition of the TiO_2 leads to an increase of T_g and a decrease in ΔT. This suggests that titanium cations have a higher impact on the bond strength of the glass network than the other elements.

The absorption spectra of the glasses are shown in figure 1a. The UV absorption edge is not clearly affected by the addition of B_2O_3 or ZnO. However, it shifts to longer wavelength with the addition of TiO_2 due to the presence of an additional broad band centered at ~500 nm which can be assigned to the absorption band of Ti^{3+} ions as suggested in [14]. In the 250-1600 nm range, several bands are observed. These bands are characteristics of the Er^{3+} ion 4f-4f transitions from the ground state to various excited levels. As seen in Figure 1b, the shape of the band centered at 1530 nm remained almost unchanged with the changes in the glass composition. One can notice that the addition of the various dopants leads to a similar increase in the absorption coefficient at 1530 nm as compared to the reference Er glass (x=0). The absorption cross-sections at 980nm and 1530 nm were measured from the absorption coefficient using equation 1 (Table 1). Within the accuracy of the measurement, the addition of the dopant in the phosphate glass has no noticeable impact on the absorption cross-sections at 1530nm. A small decrease of the absorption cross-section at 980nm was observed with the addition of TiO_2. Based on those small changes in the absorption cross-sections, the sites of the Er^{3+} ions do not seem to be strongly influenced by the changes in the glass composition.

The emission spectra after excitation at 980 nm are shown in Figure 2a. They were collected on powder between quartz plates. The spectra exhibit a broad band centered at 1530 nm which arises from the $^4I_{13/2} \rightarrow {}^4I_{15/2}$ transition typical of the Er^{3+} emission in oxide glasses. The shape of the emission band is almost unaffected by the changes in glass composition confirming the small impact of the dopants on the sites of the Er^{3+} ions (Figure 2b). As seen in Figure 2a, the addition of dopants leads to a reduction in the intensity of the emission. The larger the TiO_2 concentration, the larger the decrease in the emission intensity. This is in agreement with the small reduction in the absorption cross-section at 980nm with the addition of TiO_2 seen in Table 1. However, while the B-Er and Zn-Er glasses have similar absorption cross-sections at 980 and 1532nm than the Reference Er glass (Table 1), they exhibit a lower emission at 1532nm after 980nm excitation than the Reference Er glass. As explained in [15], the decrease of the emission at 1530nm with the addition of B_2O_3 could be due to an increase of the multiphonon decay rate by coupling of larger number of borate groups. In order to understand the emission properties of the Zn-Er glass, the IR absorption spectra the glasses were measured as the intensity of the emission at ~1530nm is related to the impurities such as OH hydroxyl groups, known as serious quenchers of Er^{3+} ions luminescence [16]. Figure 2c shows the IR absorption spectra of the glasses. The spectra exhibit a broad absorption band between 2800 and 3500 cm^{-1} which is usually attributed to OH groups in several oxide glasses [16]. No direct correlation between the OH content and the intensity of the emission at 1530nm could be established for the Zn-Er glass as this glass has the lowest amount of OH as compared to the other glasses. Therefore, it is possible to think that the addition of the ZnO in the phosphate glass changes the structure of the glass which then cannot incorporate the same amount of Er^{3+} ions than the reference Er glass without forming ions pairs. Aggregation and clustering of RE ions are known to increase the interaction between RE ions which results in luminescence quenching [17]. A study on the Er^{3+} solubility in the investigated glasses is in progress. We plan to provide more information about the impact on the glass composition on Er^{3+} coordination and clustering as performed in [18-19].

The structure of the investigated glasses was, then, analyzed using Raman and IR spectroscopies. The Raman spectra of the glasses are presented in Figure 3a. All spectra are normalized at the band with maximum intensity peaking at ~1175 cm^{-1}. The spectra exhibit well defined bands at ~700, 1175 and 1200-1300 cm^{-1}. Various bands appear between 800 and 1110

cm^{-1}. The bands at around 1250 and 1175 cm^{-1} is ascribed to the asymmetric and symmetric stretching of non-bridging $\nu(PO_2)$ of Q^2 groups, respectively [20-22]. The band at 700 cm^{-1} is related to the symmetric stretching of bridging ν_s(O-P-O) of Q^2 groups [23]. The same author refers the band at 1020 cm^{-1} as relevant of the stretching ν(P-O) of terminal groups (Q^1). From the spectra of the glasses, the investigated glasses are expected to have a metaphosphate structure, as suggested by [24] and many other publications. There is no Q^3 which are usually revealed at Raman Shift higher than 1300 cm^{-1} and a few amount of terminal group Q^1.

The addition of B_2O_3, TiO_2 and ZnO leads to a broadening of the main band at 1175 cm^{-1} which is assigned to the symmetric stretching of non-bridging $\nu(PO_2)$ of Q^2. This broadening is most likely related to a disordering of the phosphate network induced by the addition of B_2O_3, TiO_2 and ZnO. A shift to lower wavenumber of this band and also of the band at 700 cm^{-1} which is assigned to symmetric stretching of bridging ν_s(O-P-O) of Q^2 is observed and could be related to a modification of the iono-covalent state of the P-O bound [25] or to a mass effect of the cations surrounding the phosphate network [26]. The intensity of the bands between 900 and 1110 cm^{-1} increases with the addition of the dopants which is an indication of an increase of the Q^1 units. The increase in intensity of those bands is more visible in the spectrum of the Ti-Er glasses probably due to the formation of P-O-Ti and to the increase of the Q^1 units coordinated to titanium in the glasses [25]. In metaphosphate glass, the titanium cation is in an octahedral environment TiO_6 [27]. Titanium may even create a TiO_6 sub-network through Ti-O-Ti-O-Ti bonding. This chain structure, mentioned by Cardinal et al [28], induces vibrations which can be seen by the increase in intensity of the 900-1100 cm^{-1} band in the Raman spectra. Since the progressive addition of TiO_2 leads to an increase in T_g, it is possible that the formation of P-O-Ti linkages distorts the glass network and forms three-dimensional network of P-O-Ti linkages as suggested in [14]. In the Raman spectrum of the B-Er glass, the bands in the 600-650 cm^{-1} and 1050-1150 cm^{-1} range can also be related to ring-type metaborate units and diborate group, respectively. In agreement with [29], the bands in the 1050-1150cm^{-1} range can be also related to the symmetric stretching vibration $\nu(A_1)$ of the $[PO_4]^{3-}$ tetrahedron surrounded by B^{3+} ions (PO_4-BO_4 groups). According [30], the B cations are thought to enter in the phosphate network in BO_4^- tetrahedra, which share oxygen with the phosphate network. The negative charge surrounding the tetragon is then compensated by a positive charge, certainly carried by Na^+. In that case, the sodium ions around the boron units have less impact on the phosphate network leading the shift

of the Q^2 bands the in Raman spectrum. As the addition of B_2O_3 was found to also increase the T_g of the glass, the increase in connectivity cannot be due to the increase of the P-O-P bonds as the number of such bonds decreases. The increase in T_g is therefore likely to be due to the formation of P-O-B links which replace the P-O-P bonds as seen in [31]. The formation of the P-O-B links is also suggested by the increase in intensity of the shoulder at 630 cm^{-1} which is related to the vibrations of metaborate units bonded to P-O as in [32].

The IR spectra of the glasses are presented in Figure 3b. The spectra are normalized to the band with maximum intensity peaking at ~880 cm^{-1}. The spectra exhibit bands between 650 and 800 cm^{-1} and at ~880, 1080 and 1240 cm^{-1}. Various bands appear between 950 and 1010 cm^{-1}. The impact of the oxygen-(Er, Zn, B, Ti) vibrations on the bands in the low wavenumber range [33] is insignificant as compared to that of the phosphate vibrations and will not be discussed in this paper. The bands at around 1240 cm^{-1} is ascribed to the asymmetric stretching mode $\nu_{as}(PO_2^-)$ of Q^2 groups [23]. The shoulder at 1160 cm^{-1} was assigned by Meyer et al. [24] as symmetric modes (PO_2^-) of the Q^2 groups. The band at 1080 cm^{-1} is related to asymmetric stretching mode of Q^1 group, $\nu_{as}(PO_3^{2-})$ [34]. The band at 880 cm^{-1} corresponds to the asymmetric vibrational modes ν_{as}(POP) of P–O–P bridges of Q^2 units in chains [23]. The various bands between 930 and 1010 cm^{-1} are often related to rings-type formation in the glass network [35]. The broad bands between 650 and 800 cm^{-1} may include symmetric vibrational modes ν_s(POP) of P–O–P bridges of Q^2 units [23]. No bands are revealed at higher wavenumbers than 1300 cm^{-1}, where the ν(P=O) of Q^3 groups typically locate. This confirms that there are no Q^3 groups in the experimental glasses in this work, in agreement with the analysis of the Raman spectra.

The addition of B_2O_3, TiO_2 and ZnO leads to a decrease in intensity and a shift to lower wavenumber of the IR band at 1240cm^{-1} and also to an increase in intensity of the bands in the 930-1010 cm^{-1} range indicating an increase of ring structure amount into the glasses. The bands in the 930-1010 cm^{-1} range in the IR spectrum of the B-Er glass can be also related to the creation of P-O-B-O-P as discussed in the previous paragraph. The decrease in intensity of the IR band at 1085 cm^{-1} seen with the incorporation of B_2O_3 and TiO_2 might be related to the decrease of non-bridging oxygen probably due to the formation of P-O-B and P-O-Ti bonds. However, the addition of ZnO increases the intensity of this band at 1085cm^{-1} indicating an increase in Q^1 units at the expense of the other Q^n units. Zn is then suspected to act as a modifier, leading to a depolymerization of the phosphate network and to a less cross-linked network. This is in

agreement with the low density and T_g of the Zn-Er glass as compared to the other glasses. It is possible to think that it is this change in the glass structure induced by the incorporation of Zn which reduces the emission at 1530nm of the glass.

3.2 Effect of the partial crystallization on the structural and luminescence properties of the glasses

All glasses were heat treated first at their respective (T_g+20°C) for 6 and 17h followed by a hold at their respective (T_p-40°C) for 10, 30 and 60min. The duration of the heat treatments was chosen based on the study of the crystallization mechanism of the glasses with the composition $50P_2O_5$-(40-x)CaO-xSrO-$10Na_2O$ (in mol%) with x=0, 20 and 40 [10]. It was found that all these glasses when heat treated above (T_p-40°C) for 30 minutes or more were fully crystallized. Two phases were found to crystallize in the glass with x=20: $(Ca,Sr)(PO_3)_2$ and $Na(Ca,Sr)(PO_3)_3$.

No visible sign of crystallization could be seen in any investigated glasses after 10 min at their respective (T_p-40°C). The reference Er-glass became opaque after at least 30min at (T_p-40°C), which is a clear sign of crystallization. The B-Er, Zn-Er and Ti2.5-Er glasses became translucent after 60min at their respective (T_p-40°C), whereas the Ti5-Er glass had still a glassy appearance.

The crystalline phases were identified using an X-ray diffraction analyzer (Philips X'pert) with Cu Kα radiation (λ= 1.5418 Å). The XRD patterns of the glasses prior to and after the heat treatments are shown in Figures 4. The XRD pattern of the heat treated reference-Er glass (Figure 4a) clearly exhibits sharp peaks after the heat treatments. One can notice that the intensity of the peak increases dramatically when the duration of the heat treatment at (T_p-40°C) is increased from 10 to 30min. However, no significant impact of the increase in the duration of the heat treatment at (T_g+20°C) is seen on the intensity of the peaks. The peaks are mainly related to $NaCa(PO_3)_3$ based on [ICDD 00-023-0669] and $Sr(PO_3)_2$ based on [ICDD 00-012-0360]. As explained in the previous paragraph, similar crystals were found to precipitate in the glass with the composition $50P_2O_5$-20CaO-20SrO-$10Na_2O$ [10]. While some peaks could be seen in the XRD patterns of the B-Er and Zn-Er glasses (Figure 4b and c, respectively), no peaks could be seen in the XRD pattern of the Ti-Er glasses after 30min at (T_p-40°C) (Figures 5d and e). The number and intensity of the peaks seen in the XRD pattern of the B-Er and Zn-Er glasses

after 30min at (T_p-40^{o}C) are too low to identify unambiguously the crystalline phases form in the glasses. This clearly shows that the addition of the B, Zn and Ti dramatically reduces the crystallization rate. As seen in Figures 5b, c and d, an increase in the duration of the heat treatment at (T_p-40^{o}C) from 30 to 60 min leads to an increase in intensity of the peaks in the XRD patterns of the B-Er and Zn-Er glasses. Peaks appear in the XRD pattern of the Ti2.5-Er glass whereas no peaks can be seen in the XRD pattern of the Ti5-Er glass (Figure 4e). At least two phases are suspected to crystallize in the partially crystallized glasses. $NaCa(PO_3)_3$ is suspected to precipitate in all partially crystallized compositions. $Sr(PO_3)_2$ is thought to be the second phase precipitating in the Zn-Er and Ti2.5-Er glasses and $Ca_2P_2O_7$ in the B-Er glass based on [00-009-0345].

Figure 5 present the SEM images of the investigated glasses after heat treatment, polished from the side, with the external surface at the top of the image. Clear signs of surface crystallization can be seen. Similar surface crystallization was observed in the glasses within the same glass system [10]. In all samples, crystals form a layer growing from the surface. The thickness of the crystallized layer increases with the duration of the heat treatment at (T_p-40^{o}C) as seen in [10]. It is interesting that the Zn-Er glass behaves in a similar manner as the reference Er glass: after 10 minutes at (T_p-40^{o}C), large crystals with a needle like shape could be evidenced. The only difference between the reference Er and Zn-Er glasses is that the crystals grew faster in the reference Er glass. The crystals precipitating in the B-Er and Ti-Er glasses grew dendritically and slower than the crystals in the reference Er glass. A large number of small crystals are seen in the B-Er and Ti-Er glasses after 60min at (T_p-40^{o}C) (Figure 5).

From the analysis of the XRD patterns and of the SEM pictures of the heat treated glasses, it seems like the reference Er glass is the most sensitive glass to crystallization, while the Ti5-Er glass is the least sensitive composition of the experimental glasses. This difference in the crystallization tendency of the glasses can be related to the different structure of the glasses:

i) the addition of Zn ions, which act as modifiers, most likely reduces the amount of nucleation sites and decrease the crystallization rate.

ii) the increase in the glass connectivity induced by the formation of P-O-Ti/B links seems to delay crystallization in the B- and Ti-containing glasses. Therefore, an increase in the TiO_2 content increases the glass connectivity reducing further the glass crystallization tendency. This study is in agreement with [36-37]: TiO_2 was found to increase the glass stability and to promote

surface crystallization in phosphate glasses when introduced in low quantities (below 4mol%). Based on the XRD patterns of the B-Er glass, we suspect the crystals to precipitate already at the surface after 30min at (T_p-40^{o}C). The absence of crystals in the SEM micrograph of the B-Er glass heat treated 30min at (T_p-40^{o}C) might be due to inhomogeneity of the crystals precipitation.

The intensities of the emission at 1530 nm of the glasses prior to and after the heat treatments are shown in Figure 6. Bulk samples were used to collect the emission from the crystals-containing surface when using an excitation at 980nm. No increase in the emission intensity was observed after the different heat treatments. We observed a significant decrease in the intensity of the emission from the reference Er glass after 30min at (T_p-40^{o}C). When the duration of the heat treatment increased to 60min, the intensity of the emission continued to slightly decrease. A slight decrease in the emission intensity was also observed after the heat treatment of the Zn-Er glass, while no noticeable change in the emission intensity was detected for the B-Er and Ti-Er glasses. Surprisingly, all the glasses heat treated for 60min at (T_p-40^{o}C) exhibited similar emission intensity within the accuracy of the measurement. As seen in Figure 7, the shape of the emission band of Er^{3+} in the reference Er glass changed after the heat treatment indicating that changes in the sites of the Er^{3+} ions in the glass occur during the formation and growth of the crystals. However, no significant changes in the emission band shape could be noticed after heat treatment of the other glasses indicating that the crystals precipitation in B-Er, Ti-Er and Zn-Er glasses has no impact on the sites of the Er^{3+} ions. Additionally, no sharp peaks can be seen in any of the emission spectra indicating that the crystals precipitating in all the investigated glasses are Er^{3+} ions free. The Er^{3+} ions are, therefore, suspected to remain in the glass matrix.

4. **Conclusion**

The effect of the composition on the crystallization behavior of Er containing glasses in the system P_2O_5-CaO-SrO-Na_2O was investigated. Using Raman and IR spectroscopies, we suspect

i) B_2O_3 to lead to a cross-linking between the metaphosphate chains through the formation of P-O-B links.

ii) TiO_2 to form P-O-Ti linkages distorting the glass network and forming three-dimensional networks of P-O-Ti linkages

iii) ZnO to act as a modifier leading to the depolymerization of the phosphate network and to a less cross-linked network.

However, while B_2O_3, TiO_2 and ZnO have a noticeable impact on the glass structure, they do not have a significant impact of the absorption and emission properties of Er^{3+}.

The glasses were heat treated at their respective (Tg+20°C) for 6 to 17 h and at their respective (Tp-40°C) from 10 to 60 min. The glass, used as a reference, and the Ti-containing glasses are, respectively, is the most and least sensitive glass to crystallization. Two different crystals, the composition of which depends on the glass composition, are suspected to precipitate in the glasses. $NaCa(PO_3)_3$ is thought to be one of the crystals to precipitate in all glasses. A reduction in the Er^{3+} emission intensity was observed after heat treatment and from the absence of sharp peak in the Er^{3+} emission band, we suspect the Er^{3+} ions to remain in the glassy matrix in the partly crystallized samples.

With this study, we clearly show that the transformation of an Er^{3+} doped glass into glass-ceramic via nucleation and growth process does not necessarily lead to an increase in absorption and emission cross-section of rare-earth as seen in many papers. Therefore, it is crucial to continue to investigate the impact of the crystal precipitation on the rare-earth spectroscopic properties in different glass systems to further understand how to control the crystalline environment around the rare-earth ion for the crystals to actually act as effective rare- earth sensitizers.

Acknowledgments

The Magnus Ehrnrooth foundation and the Academy of Finland (grant for J. Massera and for L. Petit "Competitive Funding to Strengthen University Research Profiles; funded by Academy of Finland, decision number 310359) are gratefully acknowledged.

References

[1] M.J. Dejneka, Material Research Society Bulletin 23 (1998) 57-62.

[2] W.J. Miniscalco, J. Lightwave Technology, 9 [2] (1991) 234-250.

[3] A. Martucci, A. Chiasera, M. Montagna, M. Ferrari, Journal of Non-Crystalline Solids, 322 (2003) 295-299.

[4] C.I. Oppo, R. Corpino, P.C. Ricci, M.C. Paul, S. Das, M. Pal, S.K. Bhadra, S. Yoo, M.P. Kalita, A.J. Boyland, J.K. Sahu, P. Ghigna, F. d'Acapito, Optical Materials, 34 (2012) 660–664.

[5] R. Peretti, A.M. Jurdyc, B. Jacquier, W. Blanc, B. Dussardier, Optical Materials 33 (2011) 835.

[6] J.A. Capobianco, J.C. Boyer, F. Vetrone, A. Speghini, M. Bettinelli, Chemistry of Materials 14 (2002) 2915.

[7] Z. Yao, Y. Ding, T.Nanba, and Y. Miura, Material Science Research International, 4 [3] (1998) 141–147.

[8] L.L. Kukkonen, I.M. Reaney, D. Furniss, A.B. Seddon, Phys. Chemistry of Glasses 42 (2001) 265-273.

[9] G. Dantelle, M. Mortier, D. Vivien, G. Patriarche, Optical Materials, 28 (2006) 638-642.

[10] J. Massera, M. Mayran, J. Rocherullé, L. Hupa submitted to Journal of Material Science.

[11] G. Carl, T. Hoche, and B. Voigt, Phys. Chem. Glasses, 43C, 256–8 (2002).

[12] P. Yaowakulpattana, S. Kondo, K. Kadono and T. Wakasugi, Journal of the Ceramic Society of Japan,123 [2] (2015) 96-99

[13] J. Schwarz, H. Ticha, L. Tichy, R. Mertens, Journal of Optoelectronic and Advanced Materials, 6 (2004) 737.

[14] H. Segawa, N. Akagi, T. Yano, S. Shibata, Journal of the Ceramic Society of Japan, 118 (2010) 278-282.

[15] L. Petit, T. Cardinal, J.J. Videau, G. LeFlem, Y. Guyot, G. Boulon, M. Couzi and T. Buffeteau, J. Non-Cryst. Solids, 298 (1) (2002) 76-88

[16] Y. Yan, A.J. Faber, H. Waal, Journal of Non-Crystalline Solids, 181 (1995) 283-290.

[17] X. Feng, S. Tanabe, T. Hanada, Journal of Applied Physics 89 (2001) 3560-3567.

[18] R. S. Quimby, W. Miniscalco, B. Thompson, Journal of Applied Physics, 76(8) (1994) 4472 - 4478

[19] Z.A.S. Mahraz, M.R. Sahar, S.K. Ghoshal, M. Reza Dousti, Journal of Luminescence 144 (2013) 139–145

[20] S. Lee, A. Obata, T. Kasuga, Journal of the Ceramic Society of Japan, 117 (2009) 935-938.

[21] M.A. Karakasside, A. Saranti, I. Koutselas, Journal of Non-Crystalline Solids, 347 (2004) 69-79.

[22] A.G. Kalampounias, Journal of Physics and Chemistry, 73 (2012) 148-53.

[23] I. Konidakis, C-PE. Varsamis, EI. Kamitsos, D. Möncke, D. Ehrt, Journal of Physical Chemistry, 114 (2010) 9125-9138.

[24] K. Meyer, Journal of Non-Crystalline Solids, 209 (1997) 227-239.

[25] R. K. Brow, D. R. Tallant, W.L. Warren, A. McIntyre, D.E. Day, Phys. Chemistry of Glasses, 38 (1997) 300-306.

[26] L.L. Velli, CP.PE. Varsamis, E.I. Kamistos, D. Moncke, D. Ehrt, Physics and chemistry of Glasses, 46 2 (2005) 178-181.

[27] N. Nowak, T. Cardinal, F. Adamietz, M. Dussauze, V. Rodriguez, L. Durivault-Reymond, C. Deneuvilliers, J.E. Poirier, Materials Research Bulletin, 48 (2013) 1376-1380.

[28] T. Cardinal, E. Fargin, G. Le Flem, Journal of Solid State Chemistry, 120 (1995) 151-156.

[29] J. Yifen, C. Xiangsheng, H. Xihuai, Journal of Non-Crystalline Solids, 112 (1989) 147

[30] J.F. Ducel, J.J. Videau, M. Couzi, Physics and Chemistry of Glasses, 34 5 (1993), 212-218.

[31] D. Carta, D. Qiu, P. Guerry, I. Ahmed, E. A. Abou Neel, J. C. Knowles, M. E. Smith, R. J. Newport, Journal of Non-Crystalline Solids, 354 (2008) 3671-3677

[32] B.N. Meera, J. Ramakrishna, Journal of Non-Crystalline Solids, 159 (1993) 1

[33] R.K. Brown, Journal of Non-Crystalline Solids, 263&264 (2000) 1-28.

[34] S. Bruni, F. Cariati, D. Narducci, Vibrational Spectroscopy, 7 2 (1994), 169-173.

[35] J.A. Wilder, J.E. Shelby, Journal of the American Ceramic Society, 67 6 (1984), 438-444.

[36] Y.Nan, E. Williams, P.F. James, Journal of the American Ceramics, 75 (1992) 1641-1647.

[37] J. Popisil, P. Mosner, L. Koudelka, Journal of thermal Analysis, 84 (2006) 479-482.

Table Caption

Table 1: Density, thermal and optical properties of Er doped glasses

Table 1
Density, thermal and optical properties of Er doped glasses.

	Dopant concentration (mol%)	Density (g cm^{-3}) ± 0.02 g cm^{-3}	T_g (°C) ±3 °C	T_p (°C) ±3 °C	ΔT T_p - T_g ±6 °C	n(Erbium) (ions/cm^3) ± 4%	Absorption cross-section at 980 nm(cm^2) ±10%	Absorption cross-section at 1532 nm(cm^2) ±10%
Reference Er	0	2.85	444	664	220	7.81×10^{19}	1.52×10^{-21}	4.11×10^{-21}
B–Er	2.5mol% B_2O_3	2.89	457	680	223	7.80×10^{19}	1.91×10^{-21}	4.39×10^{-21}
Zn–Er	2.5mol% ZnO	2.88	406	641	235	7.75×10^{19}	1.54×10^{-21}	4.41×10^{-21}
Ti2.5-Er	2.5mol% TiO_2	2.86	460	661	201	7.70×10^{19}	1.16×10^{-21}	4.44×10^{-21}
Ti5–Er	5mol% TiO_2	2.88	473	681	208	7.61×10^{19}	1.29×10^{-21}	4.50×10^{-21}

Figure caption

Figure 1: Absorption spectra (a) and absorption band centered at 1530nm (b) of the investigated glasses

Figure 2: Emission (a), normalized emission (b) and IR absorption (c) spectra of the investigated glasses

Figure 3: Raman (a) and IR (b) spectra of the investigated glasses.

Figure 4: X-Ray Diffraction patterns of the glasses prior to and after heat treatment (a: Reference Er, b: B-Er, c: Zn-Er, d: Ti2.5-Er and e:Ti5-Er glasses) (* $NaCa(PO_3)_3$, $+Ca_2P_2O_7$ and – $Sr(PO_3)_2$)

Figure 5: SEM images of the cross-section of the glasses after heat treatment (note: the dark round spots are bubbles in the glass)

Figure 6: Intensity of the emission at 1.5μm intensity of the glasses as a function of the heat treatment

Figure 7: Normalized Emission spectra of the glasses prior to and after heat treatment

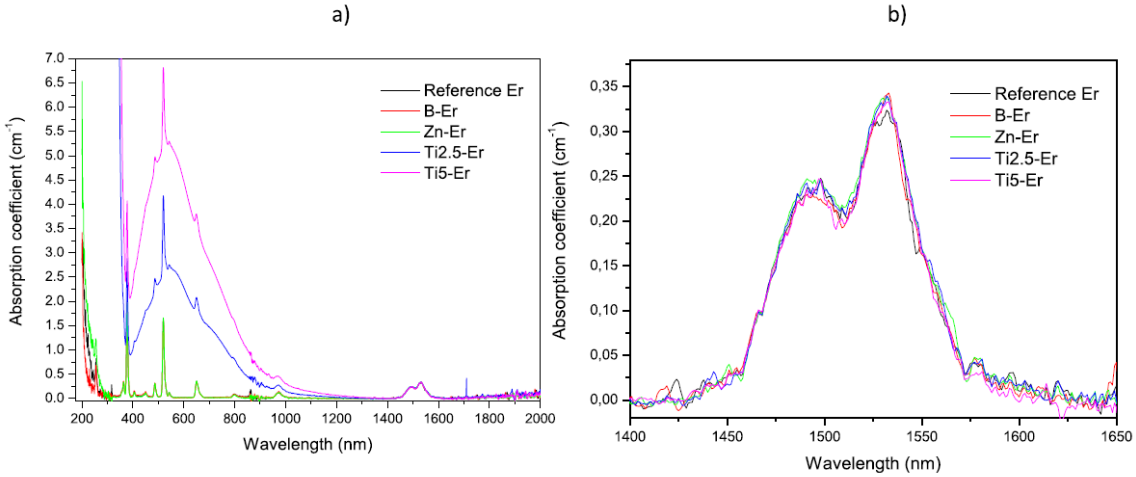

Fig. 1. Absorption spectra (a) and absorption band centered at 1530 nm (b) of the investigated glasses.

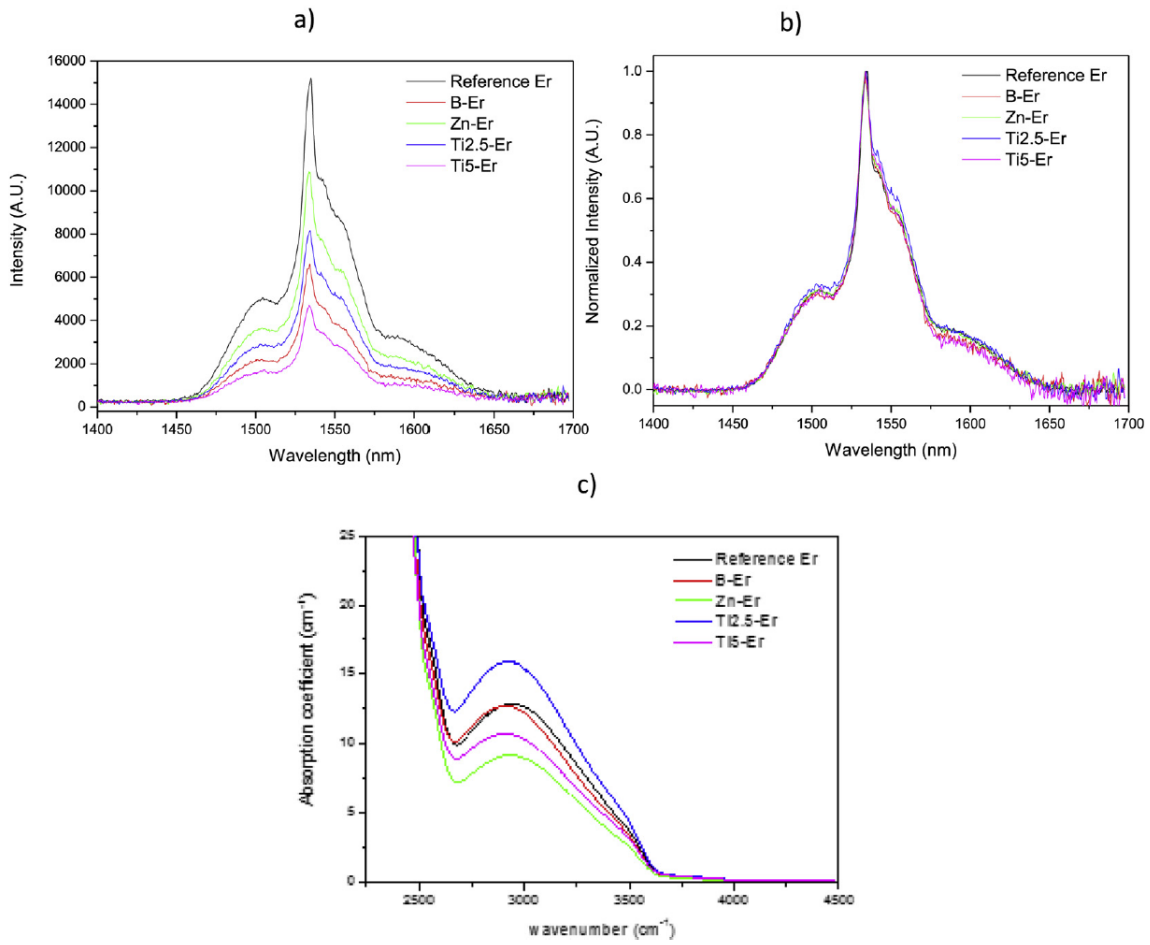

Fig. 2. Emission (a), normalized emission (b) and IR absorption (c) spectra of the investigated glasses.

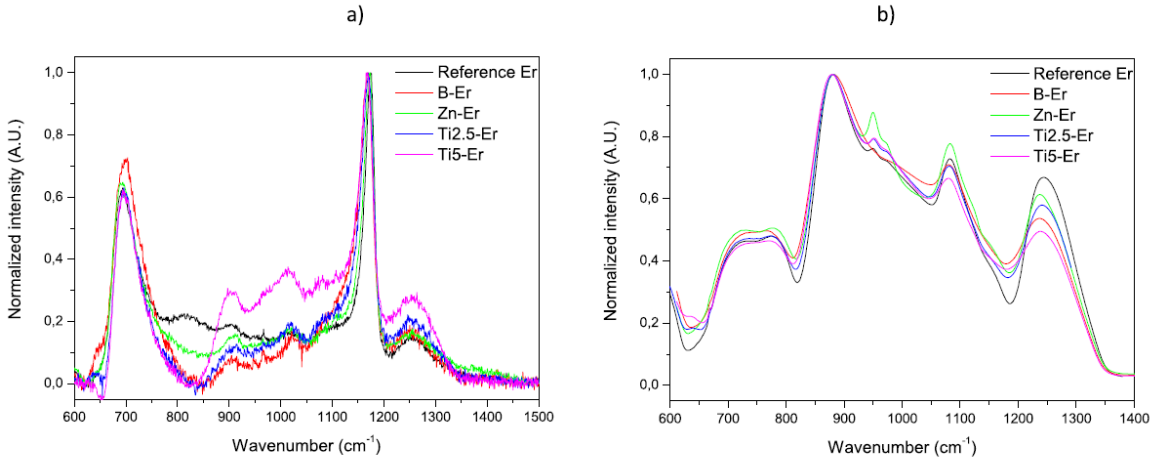

Fig. 3. Raman (a) and IR (b) spectra of the investigated glasses.

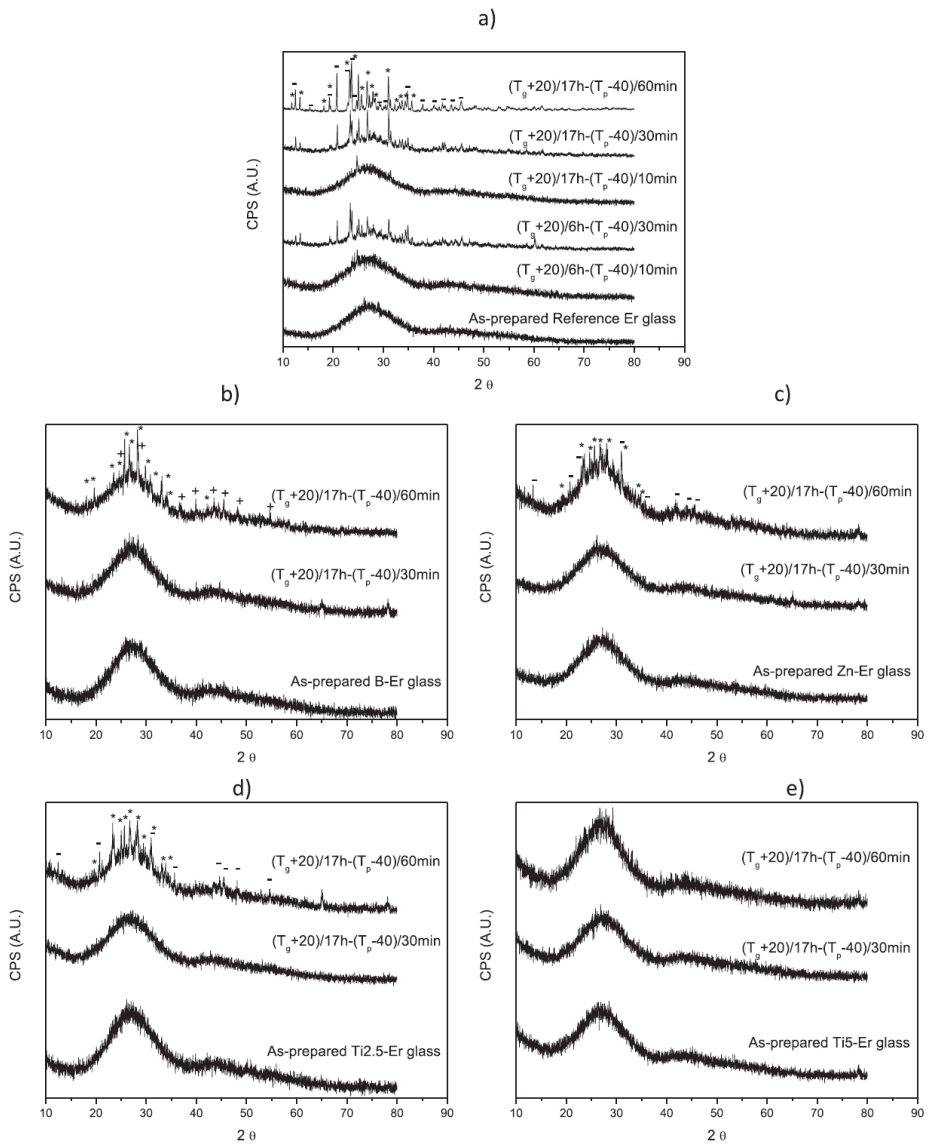

Fig. 4. X-Ray Diffraction patterns of the glasses prior to and after heat treatment (a: Reference Er, b: B–Er, c: Zn–Er, d: Ti2.5-Er and e:Ti5–Er glasses) (* $NaCa(PO_3)_3$, + $Ca_2P_2O_7$ and – $Sr(PO_3)_2$).

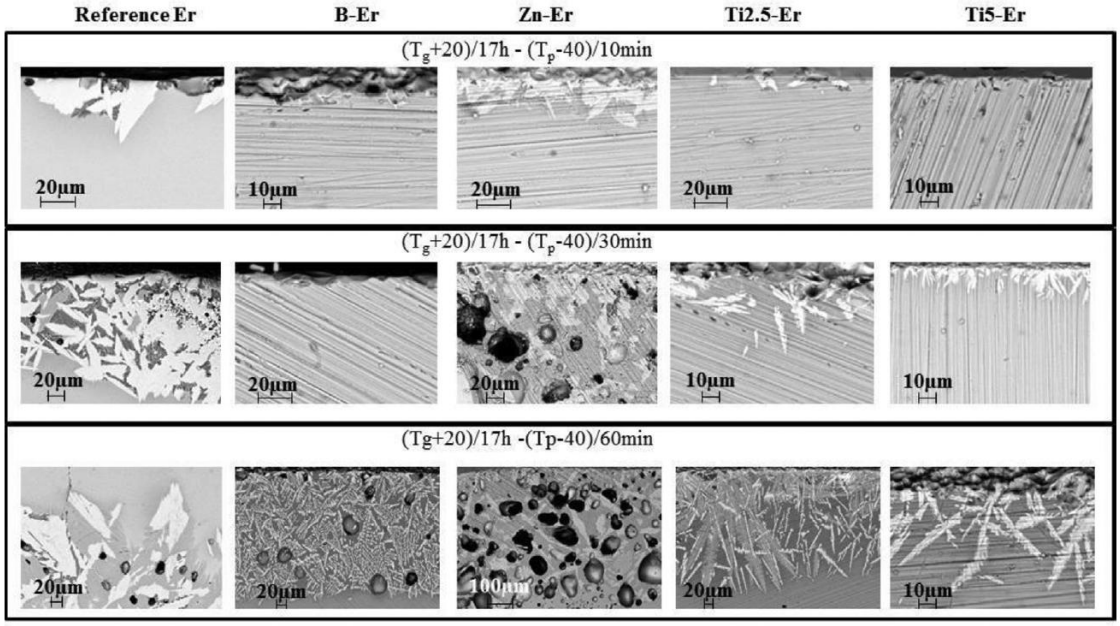

Fig. 5. SEM images of the cross-section of the glasses after heat treatment (note: the dark round spots are bubbles in the glass).

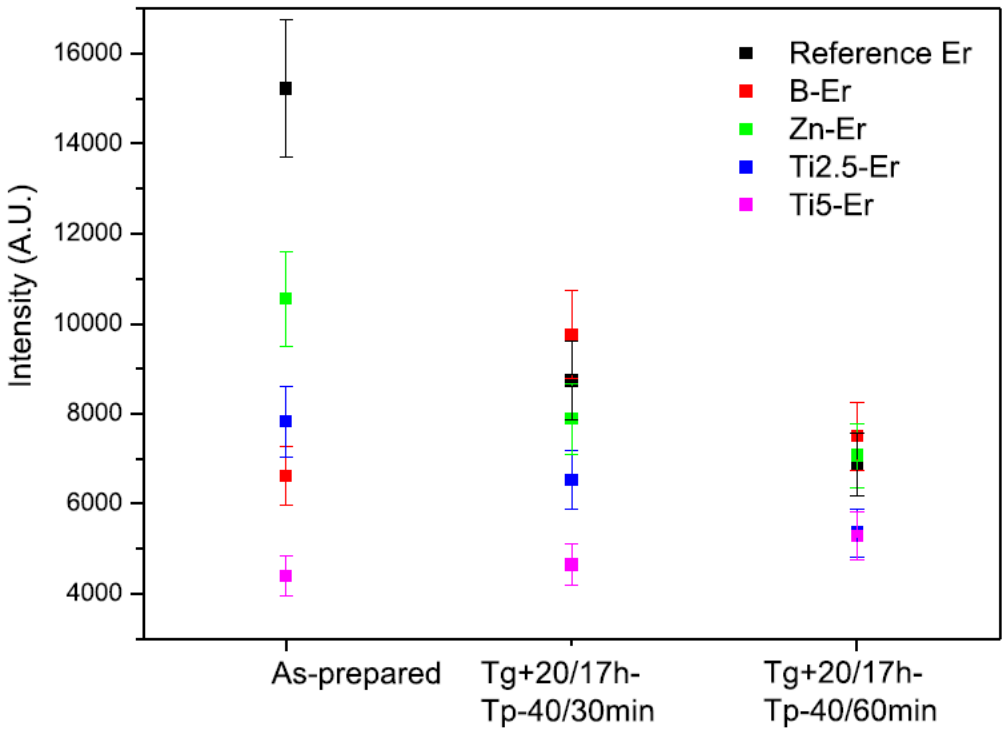

Fig. 6. Intensity of the emission at 1.5 μm intensity of the glasses as a function of the heat treatment.

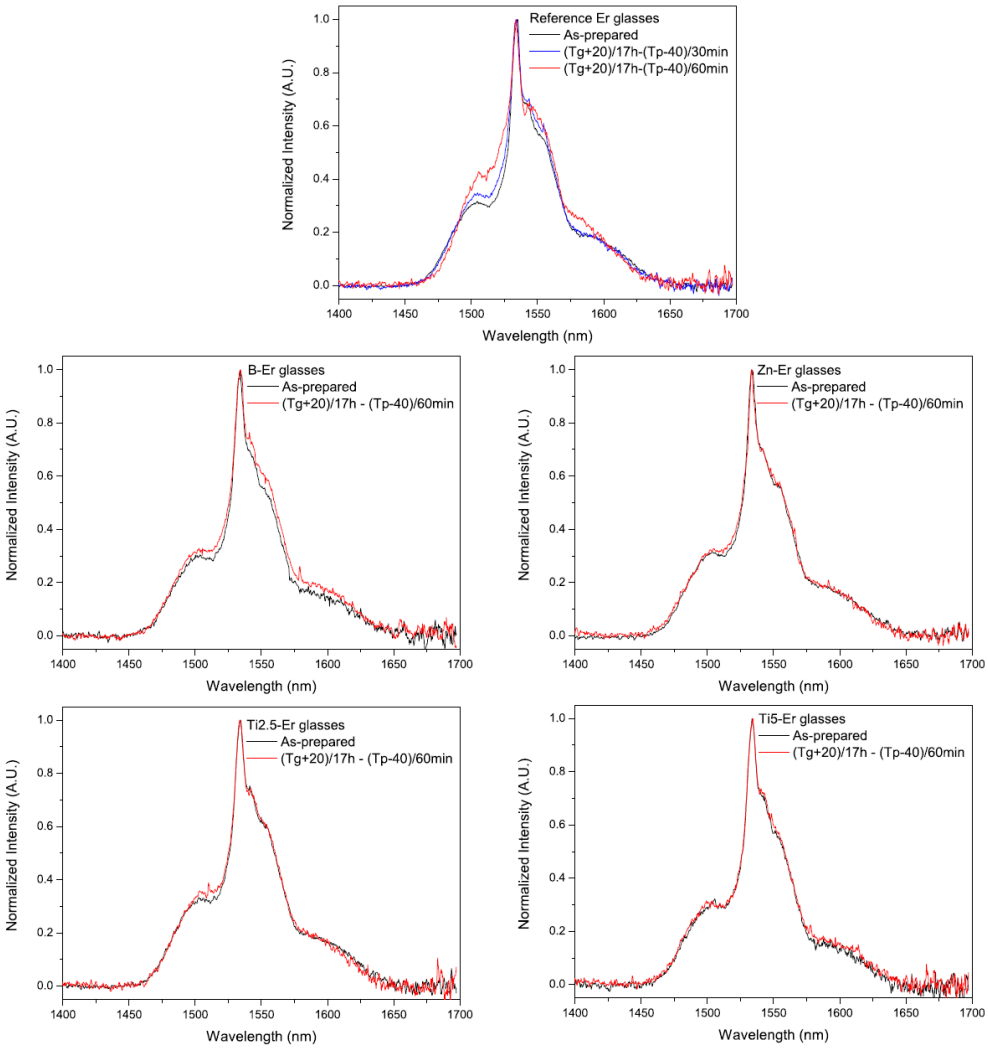

Fig. 7. Normalized Emission spectra of the glasses prior to and after heat treatment.